
Why CH_3CH_3^+ Formation Competes with H^\cdot Loss from CCCO $\text{C}_3\text{H}_6\text{O}^+$ Isomers

Charles E. Hudson and David J. McAdoo

Marine Biomedical Institute, University of Texas Medical Branch, Galveston, Texas, USA

Lawrence L. Griffin

Department of Marine Sciences, Texas A & M University at Galveston, Galveston, Texas, USA

John C. Traeger

Department of Chemistry, La Trobe University, Victoria, Australia

How formation of CH_3CH_3^+ competes with H^\cdot loss from $\text{C}_3\text{H}_6\text{O}^+$ isomers with the CCCO framework has been a puzzle of gas phase ion chemistry because the first reaction has a substantially higher threshold and a supposedly tighter transition state. These together should make CH_3CH_3^+ formation much the slower of the two reactions at all internal energies. However, the rates of the two reactions become comparable at about 20 kJ mol^{-1} above the threshold for CH_3CH_3^+ formation. It was recently shown that losses of atomic fragments increase in rate much more slowly with increasing internal energy than do the rates of competing dissociations to two polyatomic fragments. This occurs because fewer frequencies are substantially lowered in transition states for the former type of reaction than for the latter. The resulting lower transition state sums of states cause the rates of dissociations producing atoms as fragments to increase much more slowly than competing processes with increasing energy. Here we show that this is why CH_3CH_3^+ formation competes with H^\cdot loss from $\text{CH}_3\text{CH}_2\text{CHO}^+$. These results further establish that the dependence on energy of the rate of a simple unimolecular dissociation is usually directly related to the number of rotational degrees of freedom in the products, a newly recognized factor in determining the dependence of unimolecular reaction rates on internal energy. (J Am Soc Mass Spectrom 2003, 14, 136–142) © 2003 American Society for Mass Spectrometry

In 1983 Bombach and coworkers suggested that the formation of CH_3CH_3^+ by losses of CO from both ionized allyl alcohol and ionized cyclopropanol does not compete with the other primary fragmentations of those ions “in the sense of the statistical theory of unimolecular reactions” [1]. Although it is an enduring issue, there are very few clear violations of statistical theory in gas phase ion chemistry [2–5]; thus candidate examples thereof are of substantial interest. Bombach and associates concluded that, contrary to their observations, the rate of H^\cdot loss should exceed the rate of CH_3CH_3^+ formation by several orders of magnitude at the threshold for the latter because they assumed a considerably looser transition state for the former and knew its onset to be substantially lower (the thermochemical threshold is 80 kJ mol^{-1} lower according to the most recent 298 K heats of formation ($\Delta_f\text{H}(\text{CH}_3\text{CH}_3^+) = 1028 \text{ kJ mol}^{-1}$, $\Delta_f\text{H}(\text{CO}) = -110.5 \text{ kJ}$

mol^{-1} , $\Delta_f\text{H}(\text{H}^\cdot) = 218 \text{ kJ mol}^{-1}$) [6] and $\Delta_f\text{H}(\text{CH}_3\text{CH}_2\text{CO}^+) = 619.6 \text{ kJ mol}^{-1}$ [7]). This difference is lowered to 50 kJ mol^{-1} by a 30 kJ mol^{-1} reverse activation energy for H^\cdot loss from $\text{CH}_3\text{CH}_2\text{CHO}^+$ [8]. Bombach and coworkers speculated that involvement of the first electronic A state of the 1,2-epoxypropane ion might produce CO elimination from cyclopropanol and allyl alcohol ions. Dannacher and Stadelmann recently extended these views [9], suggesting that the inferred non-RRKM behavior of $\text{C}_3\text{H}_6\text{O}^+$ isomers with the CCO frame might be due to formation of CH_3CH_3^+ by an electronic predissociation, or perhaps in some way might be caused by CH_3CH_3^+ formation through an ion-neutral complex. They concluded that the electronic state of the dissociation step is common among the initial isomers considered. This is consistent with many reports demonstrating that these isomers interconvert extensively and decompose from the same precursor at low energies [8, 10–16]. Recent theoretical studies by our group demonstrate that CH_3CH_3^+ is indeed formed from $\text{C}_3\text{H}_6\text{O}^+$ isomers through an ion-neutral complex, but on the ground state manifold of that potential surface [10]. Therefore, an explanation

Published online January 10, 2003

Address reprint requests to Dr. D. J. McAdoo, Marine Biomedical Institute, University of Texas Medical Branch, 301 University Blvd., Galveston, TX 77555-1043, USA E-mail: djmcardoo@utmb.edu

other than participation of an excited electronic state is needed for the competitiveness of the two reactions.

We recently discovered that the rates of losses of atoms from ions in the gas phase generally increase much more slowly with increasing internal energy than do the rates for competing losses of polyatomic fragments [17–19]. The rates of losses of atoms are slower at higher energies for the following reason. When a transition state is located close to its dissociation products in energy, as is usually the case in simple bond cleavages, that transition state resembles the dissociated partners. The number of rotational degrees of freedom for an atom plus a polyatomic fragment is three less than the number for two polyatomic fragments (two less if one polyatomic fragment is linear, as is the case in one of the reactions considered here). Since frequencies of incipient rotations are generally much lower than vibrational frequencies, more frequencies are markedly lowered and the associated sums of states correspondingly increased in the transition state for the loss of a polyatomic fragment versus that for losing an atom. This makes the rate of production of a pair of polyatomic fragments increase much more rapidly with increasing internal energy than that of a competing loss of an atom. We show here that this is why CH_3CH_3^+ formation competes with H loss from $\text{C}_3\text{H}_6\text{O}^+$, despite the former having a substantially higher onset and the previous assumption [1] that it has a tighter transition state.

Experimental Reaction Rates

The $\text{C}_2\text{H}_6^+:\text{C}_3\text{H}_5\text{O}^+$ abundance ratio in the 70 eV mass spectrum of $\text{CH}_3\text{CH}_2\text{CHO}^+$ is 0.37 [20], demonstrating similar rates for the two reactions at higher energies. To evaluate further the competition between H loss and CH_3CH_3^+ formation, we characterized the energy dependence of those reactions by recording photoionization efficiency curves for them and then plotting the first differentials of these curves as a function of photon energy [21, 22] (Figure 1). The extent of a dissociation at the internal energy $E = h\nu - \text{IE}$ (ionization energy) is proportional to the value of the corresponding differential at that energy [21, 23]. $\text{IE} = 9.96$ eV for $\text{CH}_3\text{CH}_2\text{CHO}$ [24]. The differential curves show that H loss is the dominant reaction up to about 11.6 eV photon energy, but the rates of the two reactions become equal at 0.18 eV above the threshold for CH_3CH_3^+ formation (11.40 eV [10]) and remain approximately so for about another 0.15 eV. Thus, CH_3CH_3^+ formation clearly rises much faster with energy than does H loss. However, H loss increases further at higher energies, while CH_3CH_3^+ formation declines to negligible importance. We attribute the latter to very rapid dissociation to $\text{CH}_3\text{CH}_2 + \text{CHO}^+$ and/or $\text{CH}_3\text{CH}_2^+ + \text{CHO}$ at higher energies, thus preventing an intermediate ion-alkyl radical complex from existing long enough for H-transfer to occur. This behavior is typical of eliminations of neutral alkanes [25–27]. An alternate explana-

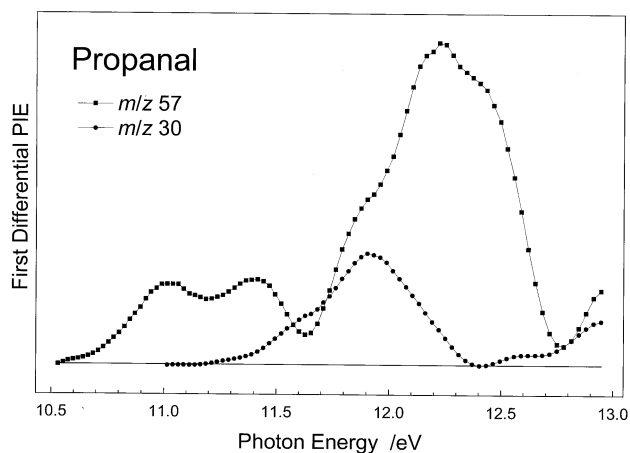


Figure 1. Plots of the first differentials of the photoionization efficiency curves for the loss of H (m/z 57) and formation of CH_3CH_3^+ (m/z 30) from $\text{CH}_3\text{CH}_2\text{CHO}^+$. The rates of the reactions at each energy are proportional to the values of the corresponding differentials at that energy.

tion might be the appearance of an additional H reaction(s) with high rates at elevated internal energies [14, 16]. However, RRKM calculations presented below make the last possibility unlikely.

Structures, Frequencies, and Energies from Theory

Structures obtained by theory [28] for the transition states for CH_3CH_3^+ formation and H loss are given in Figures 2 and 3. Structures of pertinent $\text{C}_3\text{H}_6\text{O}^+$ isomers have been published (8,10). Vibrational frequencies (Table 1) used for RRKM calculations [29] were obtained by B3LYP/6-31G(d)//B3LYP/6-31G(d) theory. Frequencies below 600 cm^{-1} were multiplied by a correction factor of 1.0013 and those above 600 cm^{-1} by

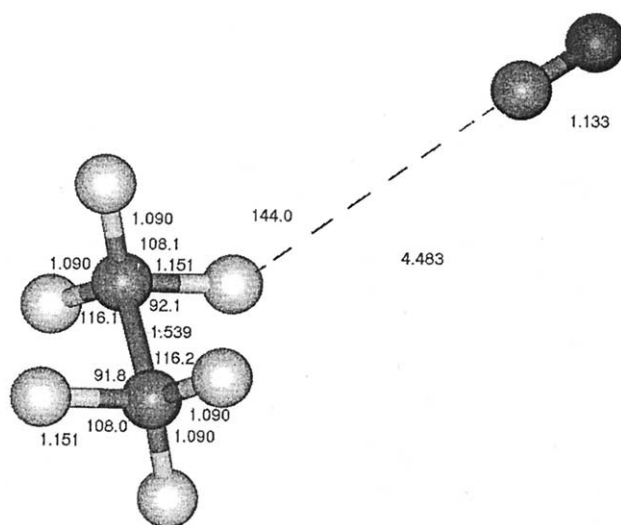


Figure 2. Geometry obtained by B3LYP/6-31G(d) theory for the transition state for the formation of CH_3CH_3^+ from $\text{CH}_3\text{CH}_2\text{CHO}^+$.

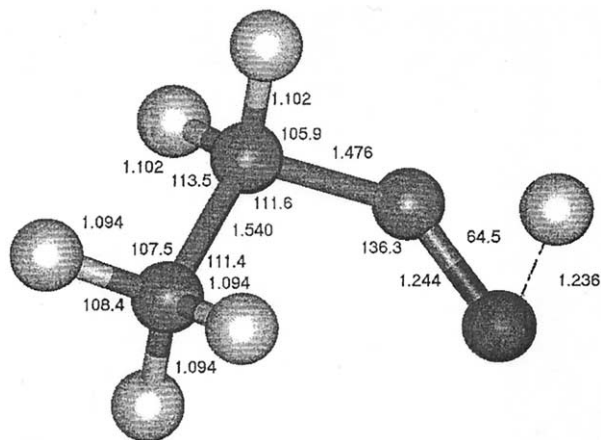


Figure 3. Geometry obtained by QCISD/6-31G(d) theory for the transition state for the loss of H[•] from CH₃CH₂CHO⁺.

0.9614 [30]. Energies of stationary points were obtained by ab initio and hybrid functional theories (Table 2). As indicated in Table 2, some of the energies were taken from a previous study of CH₃CH₃⁺ production by C₃H₆O⁺ isomers [10]. A potential energy diagram in Figure 4 summarizes pertinent reactions and ab initio energies.

The B3LYP/6-31G(d) transition state for CH₃CH₃⁺ formation is 14 kJ mol⁻¹ below the energy of the dissociated partners at the same level of theory. The

Table 1. Vibrational frequencies used in RRKM calculations

CH ₃ CH ₂ CHO ^{++a}	H [•] loss ^a	CO loss ^a	CO loss ^b
78.4	555.9i	31.9i	
244.7	130.5	7.6	100,125.0
257.2	212.8	16.9	100,125.0
475.3	224.3	55.6	100,125.0
602.5	434.9	57.3	100,125.0
630.1	493.9	233.7	230.1
833.6	603.8	414.8	391.4
876.2	755.2	519.9	620.5
981.3	779.1	645.0	700.6
1025.5	883.4	799.4	810.3
1070.3	1027.0	903.5	1041.0
1203.3	1075.0	1111.3	1105.5
1247.5	1220.8	1118.4	1122.1
1357.7	1244.1	1164.4	1182.7
1385.3	1376.2	1215.9	1207.5
1394.8	1379.8	1435.0	1427.5
1454.9	1441.6	1455.2	1447.8
1651.5	1457.0	2143.3	2123.4
2772.8	2156.0	2405.4	2515.8
2907.0	2936.0	2463.6	2564.3
2919.0	2967.6	3018.7	3044.8
2947.3	2977.3	3029.4	3049.2
3008.7	3049.4	3094.5	3127.8
3052.3	3067.5	3108.5	3136.4

^aObtained with B3LYP/6-31G(d) theory at the B3LYP/6-31G(d) geometry. All frequencies in the table are adjusted by multiplying frequencies less than 600 cm⁻¹ by 1.0013 and frequencies greater than 600 cm⁻¹ by 0.9614 [30].

^bObtained by combining B3LYP/6-31G(d) frequencies of the products with 4 125 cm⁻¹ frequencies to represent the transition modes.

potential energy must decrease in both directions from a saddle point in a reaction coordinate, so products with an energy above that of a nearby transition state imply a shallow minimum, i.e., an ion-neutral complex, between that transition state and the dissociated products. However, no effort was made to locate such a minimum. This transition state was not found in QCISD theory by moderate effort, so there may not actually be a saddle point transition state for this reaction. If the latter is so, as may often be the case for simple bond cleavages, the rate would be determined by an entropic bottleneck, i.e., the point on the reaction coordinate at which the sum of states is a minimum [31–33]. Since such entropy bottlenecks occur just below the threshold for complete dissociation of the associated reactant [32], one for CH₃CH₃⁺ formation would have frequencies and a critical energy much like those for the B3LYP/6-31G(d) transition state that we located. As expected for four vibrations and the reaction coordinate being transformed into rotations and translations, the four lowest vibrational frequencies for the B3LYP/6-31G(d) transition state leading to CH₃CH₃⁺ formation (excluding the reaction coordinate) are 4.6–14 times lower than the corresponding lowest CH₃CH₂CHO⁺ frequencies. These low frequencies arise from the C–C bond in the transition state for forming CH₃CH₃⁺ being extended to 5.457 Å.

In QCISD/6-31G(d) theory, the transition state for H[•] loss from CH₃CH₂CHO⁺ occurs at a relatively short C–H bond extension—to 1.701 Å from 1.114 Å in the ground state. The lowest frequencies in the transition state for H[•] loss are reduced at most by about 50% relative to those in CH₃CH₂CHO⁺. The four lowest frequencies in the transition state for CH₃CH₃⁺ formation are 4.0–17 times lower than the four lowest frequencies for the transition state for H[•] loss, demonstrating a much looser transition state for the first reaction. This is contrary to the supposition of Bombach and coworkers [1]. Similar frequencies were reported to be relatively unchanged in the transition state for H[•] loss from some C₄H₈⁺ isomers years ago [32], regarding which the comment was made “While saddle points and tight transition states for simple H bond fissions may appear unusual, they are not unprecedented.” In that study the transition frequencies (those that change substantially between the ground and transition state) for loss of methyl were markedly lowered.

A reverse activation energy of about 30 kJ mol⁻¹ was found for H[•] loss both here and previously [8]. Our relative energy for the products of H[•] loss, 45 kJ mol⁻¹, agrees reasonably with 60 mol⁻¹ derived by correcting heats of formation [6, 7] listed above to 0 K values using enthalpy corrections provided by theory (13.6 kJ mol⁻¹ for CH₃CH₂CO⁺, -2.0 kJ mol⁻¹ for H[•], and 16.4 kJ mol⁻¹ for CH₃CH₂CHO⁺) and combining them with Δ_fH(CH₃CH₂CHO⁺) = 772.9 kJ mol⁻¹ [6]. We believe therefore that the theoretical parameters for the transition state for that reaction are reasonable.

Table 2. Ab initio energies for dissociations of $\text{CH}_3\text{CH}_2\text{CHO}^+$

	B3LYP/6-31G(d)// B3LYP/6-31G(d)	QCISD/6-31G(d)// QCISD/6-31G(d)	QCISD(T)/6-311G(d,p)// QCISD/6-31G(d)	ZPE ^a	E (kJ mol ⁻¹) ^b
$\text{CH}_3\text{CH}_2\text{CHO}^+$ (1) ^c	-192.788003 ^d	-192.200867	-192.341978	209.5	0
$[\text{CH}_3\text{CH}_2\text{—HCO}]^+$ (2) ^c	-192.751597	-192.165020	-192.315377	193.2	54
$[\text{CH}_3\text{CH}_2\text{CHO}]^+$ (TS(1 \rightarrow 2)) ^c	-192.741115	-192.153418	-192.300832	198.4	97
TS(2 \rightarrow CH_3CH_3^+ + CO) ^e	-192.724244			185.3	
CO^c	-113.309454	-113.029616	-113.093770	13.0	
$\text{CH}_3\text{CH}_3^{+c}$	-79.410498	-79.114215	-79.193846	175.1	
CH_3CH_3^+ + CO	-192.719952	-192.143831	-192.287616	188.1	121
TS(1 \rightarrow $\text{CH}_3\text{CH}_2\text{CO}^+$ + H) ^c	-192.745239	-192.163829	-192.307253	194.2	76
$\text{CH}_3\text{CH}_2\text{CO}^+$	-192.246649	-191.680454	-191.817561	190.4	
H ^c	-0.498231	-0.498231	-0.499809		
$\text{CH}_3\text{CH}_2\text{CO}^+$ + H ^c	-192.744880	-192.178685	-192.317370	190.4	45
$[\text{CH}_2\text{CH}_2\text{CH=OH}]^+$ (3)		-192.201047	-192.343768	215.2	-10
$\text{CH}_3\text{CH=CHOH}^+$ (4)		-192.233054	-192.374860	219.8	-76
TS(1 \rightleftharpoons 3)	-192.761833	-192.167593	-192.312437	202.8	71
TS(3 \rightleftharpoons 4)		-192.173416	-192.320844	210.1	56
$\text{CH}_2=\text{CHCH=OH}^+$		-191.658214	-191.793978	193.1	
$\text{CH}_2=\text{CHCH=OH}^+$ + H ^c		-192.156445	-192.293787	193.4	110

^aValues given were obtained from those produced by B3LYP/6-31G(d) theory by multiplying by a scaling factor of 0.9806 as described in ref. 30.

^bQCISD(T)/6-311 G(d,p) energies relative to the energy of **1** = 0.

^cFrom ref. 10.

^dNot comparable to other B3LYP values because a more stringent optimization criterion was applied; this was necessary to achieve optimization.

^eBased on the B3LYP/6-31G(d) data. At this level of theory, TS(**2** \rightarrow CH_3CH_3^+ + CO) is 14 kJ mol⁻¹ below $\Delta_f\text{H}(\text{CH}_3\text{CH}_3^+) + \Delta_f\text{H}(\text{CO})$.

Reaction Rates

Since both dissociations of interest take place directly from $\text{CH}_3\text{CH}_2\text{CHO}^+$ [8, 10], we performed RRKM calculations for dissociations from that structure. These calculations appropriately characterize the competition between the loss of H[•] and formation of CH_3CH_3^+ while keeping simple the effort to define the origin of the competition at issue. Bouchoux et al. [8] suggested that choosing $\text{CH}_3\text{CH}_2\text{CHO}^+$ as the dissociating species gives RRKM rates higher than the experimental ones because the facile interconversion of CCCO $\text{C}_3\text{H}_6\text{O}^+$ isomers [8, 10–16] effectively makes the much more stable $\text{CH}_3\text{CHCH=OH}^+$ the reactant for RRKM purposes. However, we show below that this is probably not so.

The experimental PIE curve for H[•] loss approaches its onset slowly, making it difficult to extract an accurate threshold for that reaction. Therefore, we used the critical energy from Table 2 (76 kJ mol⁻¹) and the frequencies in Table 1 for RRKM calculations of rates of

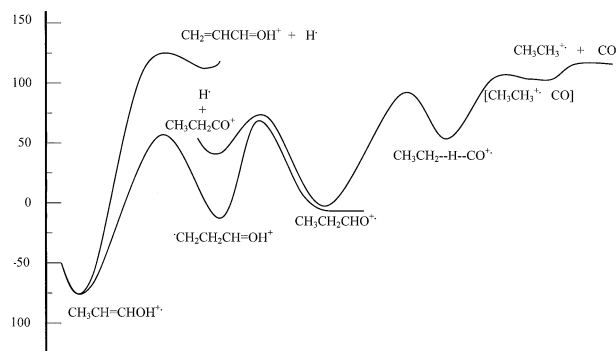


Figure 4. Potential energy diagram for the reactions of interest based on energies given in Table 2.

H[•] loss. The rate constants that we so obtained for H[•] loss from $\text{CH}_3\text{CH}_2\text{CHO}^+$ varied from 2.5×10^6 s⁻¹ near threshold to 6.1×10^{11} s⁻¹ at 178 kJ mol⁻¹ above the threshold for CH_3CH_3^+ formation (Figure 5). Corresponding rate constants obtained previously for this reaction were slightly above 10^8 s⁻¹ at threshold in one study [1] and in another they varied from 1.8×10^8 s⁻¹ to almost 1×10^{12} s⁻¹ over the energy range considered here [8]. Our rates are slower than previously obtained ones primarily because our critical energy for the reaction is higher (76 kJ mol⁻¹ versus 44 kJ mol⁻¹ [8]).

A number of models were considered for the transition state for RRKM calculations of the rate of formation of CH_3CH_3^+ . The first model used exclusively the

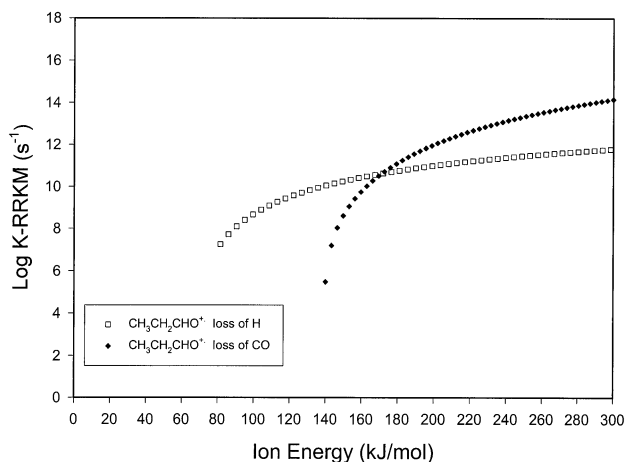


Figure 5. RRKM log k versus energy curves for the dissociations of $\text{CH}_3\text{CH}_2\text{CHO}^+$. For these RRKM calculations, a critical energy of 139 kJ mol⁻¹ and frequencies from B3LYP/6-31G(d) theory were used.

transition state frequencies produced by B3LYP/6-31G(d) theory, and published heats of formation of the species involved [6] corrected to 0 K (139 kJ mol^{-1} , see above) to provide an energy for $\text{CH}_3\text{CH}_3^{++}$ formation. Frequencies for the transition state for CO loss from the ion-neutral complex $[\text{CH}_3\text{CH}_2 \cdots \text{H} \cdots \text{CO}]^{++}$ were used because this is the actual transition state for dissociation. In this model, CO loss surpassed H loss at 29 kJ mol^{-1} above the onset of $\text{CH}_3\text{CH}_3^{++}$ formation (Figure 5). This is in the range in which the experimental rates of the two reactions are comparable (Figure 1), so this model, which is without any adjustments of its parameters, provides crossover energies in excellent agreement with experimental results.

In the second model, the vibrational frequencies of the separated products were combined with the frequencies of four symmetric top internal rotors that were assigned reduced moments of inertia as occurs in the methyl-methyl internal rotation in methane. Theoretical energies for the reactants and products (Table 2) were used to derive the critical energy, 121 kJ mol^{-1} . This transition state strongly resembles the dissociated products (Figure 2). It is considered because even though $\text{CH}_3\text{CH}_3^{++}$ is being formed by an H-transfer in an ion-neutral complex $[\text{CH}_3\text{CH}_2 \cdots \text{H} \cdots \text{CO}]^{++} \rightarrow \text{CH}_3\text{CH}_3^{++} + \text{CO}$, at this transition state, the H is transferred to the point that the ethane ion plus CO are essentially fully formed (Figure 2). Therefore, it is possible that, as assumed in this model, the developing fragments rotate fairly freely relative to each other before the dissociation limit is reached [10], a characteristic of ion-neutral complexes [34]. It is to be noted that the vibrational frequencies of the separated products correspond quite closely to the correspondingly ranked ones obtained by theory for the transition state (Table 1), supporting the plausibility of the parameters in this model. The free rotors were assigned to take into account the four vibrations other than the reaction coordinate that become rotations and translations in this dissociation. In this model, $\text{CH}_3\text{CH}_3^{++}$ formation surpasses H loss at 14 kJ mol^{-1} above the onset for the former (Figure 6), very close to the energy at which the rates of the two reactions become equal experimentally (Figure 1). This model is also in good agreement with results in Figure 1. Thus a free rotor model also appears to be accurate, suggesting that the transition state has essentially separated fragments, as indicated by its structure from theory (Figure 2).

In the third model, the frequencies of the separated products were combined with four frequencies of 100 cm^{-1} and a critical energy of 139 kJ mol^{-1} for $\text{CH}_3\text{CH}_3^{++}$ formation to test the effect of tightening the transition state. These frequencies were chosen arbitrarily, but are higher than those produced by theory (Table 1) and in the range of transition frequencies needed previously to reproduce experimental rates of alkyl losses by RRKM theory [18]. A crossover energy 160 kJ mol^{-1} above the onset of $\text{CH}_3\text{CH}_3^{++}$ formation was obtained (Figure 7), much higher than the energies at which the two rates

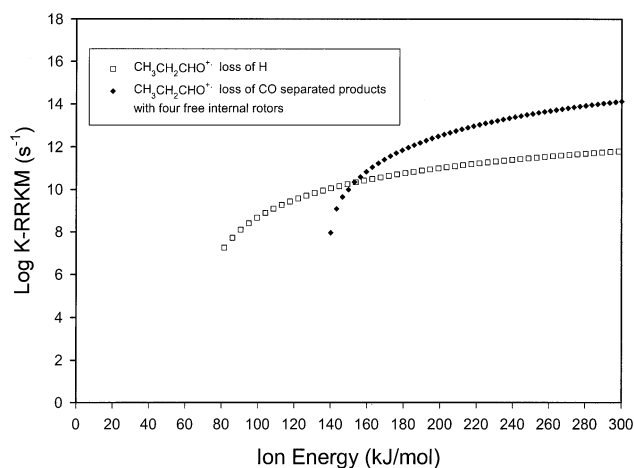


Figure 6. RRKM log k versus energy curves obtained as for Figure 5, except the four lowest B3LYP/6-31G(d) frequencies in the transition state for $\text{CH}_3\text{CH}_3^{++}$ formation were replaced with those for four incipient rotations.

come together experimentally (Figure 1). Thus, this transition state is too tight. Even so, in it the rate for loss of the polyatomic fragment still rose much faster than did the H loss rate, demonstrating that the crossover energy is also very sensitive to changes in transition state frequencies.

In a fourth model, a critical energy of 121 kJ mol^{-1} (the dissociation energy from theory) was used while retaining four 100 cm^{-1} frequencies; a crossover energy of 100 kJ mol^{-1} resulted. Thus, the crossover energy decreases dramatically with a mere 18 kJ mol^{-1} reduction in the critical energy for $\text{CH}_3\text{CH}_3^{++}$ formation. The location of the crossover points in the rate curves relative to the onset for $\text{CH}_3\text{CH}_3^{++}$ formation are thus also very sensitive to the critical energy utilized. When the four lowest frequencies were set equal to 125 cm^{-1} with a critical energy of 121 kJ mol^{-1} , the crossover energy increased to 150 kJ mol^{-1} . This further demon-

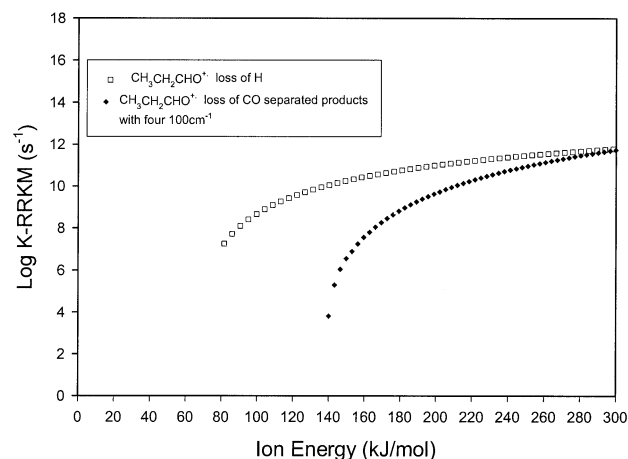


Figure 7. RRKM log k versus energy curves obtained as for Figure 5, except the four lowest B3LYP/6-31G(d) frequencies in the transition state for $\text{CH}_3\text{CH}_3^{++}$ formation were replaced with four 100 cm^{-1} frequencies.

strates that the crossover energy is also quite sensitive to the values assigned for the four transition frequencies. The first two models gave good results; modest changes in the critical energy or in the values of the transition frequencies give results in much poorer agreement with experiment. Thus the parameters that can reproduce the observed crossover energy are tightly constrained, supporting the validity of the parameters derived by theory.

It is to be noted that the pathway to CH_3CH_3^+ from $\text{CH}_3\text{CH}_2\text{CHO}^{++}$ very likely goes through a stable ion-neutral complex $[\text{CH}_3\text{CH}_2 \cdots \text{H} \cdots \text{CO}]^{++}$ [10], designated **2** in Table 2. The density of states of this complex is equal within 5% to that of $\text{CH}_3\text{CH}_2\text{CHO}^{++}$ over the entire energy range in which both reactions occur. This means that the rates of CH_3CH_3^+ formation we obtained by RRKM calculations throughout this work are probably twice higher than they should be. This would lower the corresponding log *k* curves by 0.3 units, not enough to materially affect any of our conclusions.

As already noted, our experimental results for H loss may be influenced by additional mechanisms for the loss of H at higher energies. This is not the case near threshold, as $\text{CH}_3\text{CH}_2\text{CO}^+$ is the exclusive product of H loss from metastable $\text{CCCO C}_3\text{H}_6\text{O}^{++}$ ions [13, 15] and the dominant one in the ion source at low energies [14]. However, $\text{CH}_2=\text{CHCHOH}^{++}$ is the major product of H loss from $\text{CH}_3\text{CH}=\text{CHOH}^{++}$ at higher energies [14], so a substantial contribution from that reaction is a possibility. To evaluate the extent of additional H losses, we performed RRKM calculations on the losses of H from $\text{CH}_3\text{CH}=\text{CHOH}^{++}$, $\text{CH}_2=\text{CHCH}_2\text{OH}^{++}$ and $\text{CH}_3\text{CH}_2\text{CHO}^{++}$ assuming $\text{CH}_3\text{CH}=\text{CHOH}^{++}$ to be the effective RRKM reactant, as hypothesized by Bouchoux and coworkers [8]. The energy and frequencies of $\text{CH}_3\text{CH}=\text{CHOH}^{++}$ were used for the reactant in the RRKM calculations in combination with parameters for the transition states for dissociation from each of the reactants. CH_3CH_3^+ formation treated as though it arises directly from $\text{CH}_3\text{CH}=\text{CHOH}^{++}$ still rose rapidly enough with energy to surpass all of the H losses (Figure 8). This further supports the central thesis of this work regarding the slowness of the rates of dissociations producing single atoms. In RRKM theory, taking reactions to be effectively from $\text{CH}_3\text{CH}=\text{CHOH}^{++}$ made them almost two orders of magnitude slower than corresponding ones from $\text{CH}_3\text{CH}_2\text{CHO}^{++}$ at the same energy. RRKM calculations by Bouchoux and coworkers indicate that H loss directly from $\text{CH}_3\text{CH}_2\text{CHO}^{++}$ is about two orders of magnitude faster than isomerization to $\text{CH}_2\text{CH}_2\text{CH}=\text{OH}^+$. Therefore at higher energies in the ion source H is probably lost from $\text{CH}_3\text{CH}_2\text{CHO}^{++}$ much faster than isomerization thereof, making simple cleavage the major H loss. Thus it is unlikely that this system equilibrates for the purposes of RRKM calculations. This implies that our RRKM treatment of the dissociations of interest as coming directly from $\text{CH}_3\text{CH}_2\text{CHO}^{++}$ is the most valid

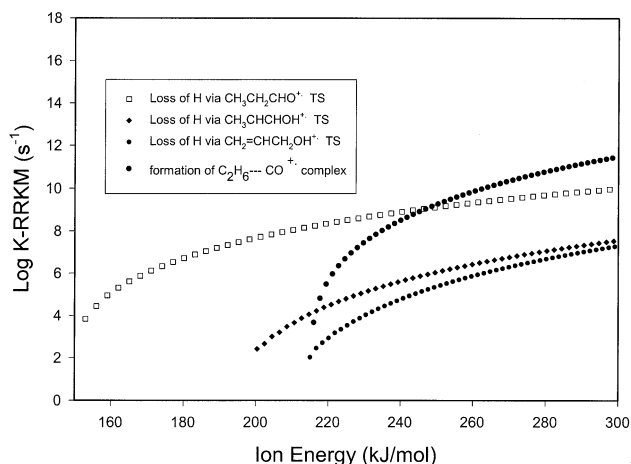


Figure 8. RRKM log *k* versus energy curves obtained by assuming that $\text{CH}_3\text{CH}=\text{CHOH}^{++}$ is the effective reactant in the dissociations of $\text{CH}_3\text{CH}_2\text{CHO}^{++}$. The reactions considered are CH_3CH_3^+ formation and H loss through transition states from $\text{CH}_3\text{CH}_2\text{CHO}^{++}$, $\text{CH}_3\text{CH}=\text{CHOH}^{++}$, and $\text{CH}_2=\text{CHCH}_2\text{OH}^{++}$. The transition state energies for corresponding reactions are the same as in Figures 5–7, but the scale is shifted by the difference between $\Delta_f\text{H}(\text{CH}_3\text{CH}_2\text{CHO}^{++})$ and $\Delta_f\text{H}(\text{CH}_3\text{CH}=\text{CHOH}^{++})$. Note that the rate constants in this plot are 1–3 orders of magnitude lower than those in Figures 5–7.

way to treat the competition between CH_3CH_3^+ formation and H loss.

All combinations of parameters used for dissociations from $\text{CH}_3\text{CH}_2\text{CHO}^{++}$ produced a much faster rise with energy of CH_3CH_3^+ formation than H loss. The range of critical energies for CH_3CH_3^+ formation used in RRKM calculations was 107 kJ mol^{-1} – 145 kJ mol^{-1} , and the frequencies were as above. (The results of some of these calculations are not given.) The fewer low frequency modes in transition states for losses of atoms versus those for losses of polyatomic fragments account for the competitiveness of the latter type of reactions with the former at suprathreshold energies, even in the face of the higher onset energies for the latter. This further supports the general occurrence of the difference between the energy dependencies of the rates of losses of atoms versus polyatomic fragments. It also extends it to a case producing a diatomic fragment having only two rather than the previously investigated dissociations to products with three rotational degrees of freedom [17–19]. Present and other recent work [17–19] add a hitherto unappreciated factor to the known determinants, simple dissociation versus rearrangement, of the dependence of unimolecular reaction rates on reactant internal energy. Simple dissociations typically increase much more rapidly in rate with increasing energy than do rearrangements.

References

- Bombach, R.; Dannacher, J.; Honegger, E.; Stadelmann, J-P. Unimolecular Dissociations of Excited $\text{C}_3\text{H}_6\text{O}^+$: A Photoelectron-Photoion Coincidence Study of Cyclopropanol and Allyl Alcohol. *Chem. Phys.* **1983**, *82*, 459–470.

- McLafferty, F. W.; McAdoo, D. J.; Smith, J. S.; Kornfeld, R. The Enolic $C_3H_6O^+$ Ion Formed from Aliphatic Ketones. *J. Am. Chem. Soc.* **1971**, *93*, 3720–3730.
- Lifshitz, C. Intramolecular Energy Redistribution in Polyatomic Ions. *J. Phys. Chem.* **1983**, *87*, 2304–2313.
- Sun, L.; Song, K.; Hase, W. L. A S_N2 Reaction that Avoids Its Deep Potential Energy Minimum. *Science* **2002**, *296*, 875–878.
- Nummela, J. A.; Carpenter, B. K. Nonstatistical Dynamics in Deep Potential Wells: A Quasiclassical Trajectory Study of Methyl Loss from the Acetone Radical Cation. *J. Am. Chem. Soc.* **2002**, *124*, 8512–8513.
- Lias, S. G.; Bartmess, J. E.; Liebman, J. F.; Holmes, J. L.; Levin, R. D.; Mallard, W. G. Gas Phase Ion and Neutral Thermochemistry. *J. Phys. Chem. Ref. Data* **1988**, *17*, 76, 97, 119, 616.
- Traeger, J. C. unpublished.
- Bouchoux, G.; Luna, A.; Tortajada, J. Rearrangement and Dissociative Processes in the $[C_3H_6O]^+$ Potential Energy Surface. Radical Cations with the CCCO Frame: A Model System. *Int. J. Mass Spectrom. Ion Processes* **1997**, *167/168*, 353–374.
- Dannacher, J.; Stadelmann, J.-P. Behavior of Excited $C_3H_6O^+$ Cations: A He-I α Photoelectron-Photoion Coincidence Study of Propanal. *Int. J. Mass Spectrom.* **2001**, *208*, 147–157.
- Hudson, C. E.; McAdoo, D. J.; Traeger, J. C. $CH_3CH_3^+$ Formation from $C_3H_6O^+$ Isomers According to Theory. *J. Am. Soc. Mass Spectrom.* **2002**, *13*, 1235–1241.
- Kurland, J. J.; Lutz, R. P. Mass Spectra of Deuterium-Labeled Allyl Alcohols: Evidence for Rearrangement of the Molecular Ion. *Chem. Commun.* **1968**, 1097–1098.
- McAdoo, D. J.; Witiak, D. N. Metastable Decomposition of $C_3H_6O^+$ Ions. *J. Chem. Soc. Perkin II* **1981**, 770–773.
- Hudson, C. E.; McAdoo, D. J. Propanoyl Ion Formation from Metastable $[C_3H_6O]^+$ Ions. *Org. Mass Spectrom.* **1982**, *17*, 366–368.
- Turecek, F.; Hanus, V.; Gäumann, T. Fast and Slow Decompositions of Ionized Propen-1-ols. A Unified View of $[C_3H_6O]^+$ Isomers with the C-C-C-O Frame. *Int. J. Mass Spectrom. Ion Processes* **1986**, *69*, 217–231.
- Polce, M. J.; Wesdemiotis, C. The Distonic Ion $CH_2CH_2CH^+OH$, Keto Ion $CH_3CH_2CH=O^+$, Enol Ion $CH_3CH=CHOH^+$, and Related $C_3H_6O^+$ Radical Cations. Stabilities and Isomerization Proclivities Studied by Dissociation and Neutralization-Reionization. *J. Am. Soc. Mass Spectrom.* **1996**, *7*, 573–589.
- Hudson, C. E.; McAdoo, D. J. β Cleavages of Distonic Ions, α Cleavages of Enol Ions, Isomerizations of Distonic and Enol Ions, and Corresponding Reactions of Free Radicals. *Int. J. Mass Spectrom.* **2001**, *210/211*, 417–428.
- McAdoo, D. J.; Olivella, S.; Solé, A. Theoretical Analysis of the Unimolecular Gas-Phase Decompositions of the Propane Molecular Ion. *J. Phys. Chem. A* **1998**, *102*, 10798–10804.
- Griffin, L. L.; Traeger, J. C.; Hudson, C. E.; McAdoo, D. J. Why Are Smaller Fragments Preferentially Lost from Radical Cations at Low Energies and Larger Ones at High Energies? An Experimental and Theoretical Study. *Int. J. Mass Spectrom.* **2002**, *217*, 23–44.
- Hudson, C. E.; Traeger, J. C.; Griffin, L. L.; McAdoo, D. J. Why do Losses of Polyatomic Fragments Strongly Dominate Losses of Atoms at High Internal Energies? Methyl Versus Cl⁻ Loss from the 2-Chloropropane Cation. *J. Phys. Chem.*, in press.
- Stenhagen, E.; Abrahamsson, S.; McLafferty, F. W. Atlas of Mass Spectra, I. Interscience Publishers: New York, 1969 p 27.
- Hurzeler, H.; Inghram, M. G.; Morrison, J. D. Photon Impact Studies of Molecules Using a Mass Spectrometer. *J. Chem. Phys.* **1958**, *28*, 76–82.
- Traeger, J. C.; Morton, T. H. Mechanisms for the Expulsion of Propene from Ionized Propyl Phenyl Ethers in the Gas Phase. *J. Am. Chem. Soc.* **1996**, *118*, 9661–9668.
- Traeger, J. C.; Hudson, C. E.; McAdoo, D. J. A Photoionization Study of the Ion-Neutral Complexes $[CH_3CH^+CH_3 \cdot CH_2CH_3]$ and $[CH_3CH_2CH^+CH_3 \cdot CH_3]$ in the Gas Phase: Formation, H-Transfer and C-C Bond Formation Between Partners, and Channeling of Energy into Dissociation. *J. Am. Soc. Mass Spectrom.* **1996**, *7*, 73–81.
- Traeger, J. C. Heat of Formation for the Propanoyl Cation by Photoionization Mass Spectrometry. *Org. Mass Spectrom.* **1984**, *20*, 223–227.
- Traeger, J. C.; Hudson, C. E.; McAdoo, D. J. Alkane Eliminations from Ionized Ketones in the Gas Phase: Dependence of Ion-Neutral-Complex-Mediated Decompositions on the Properties of the Ionic and Neutral Partners. *J. Phys. Chem.* **1988**, *92*, 1519–1523.
- McAdoo, D. J. Ion-Neutral Complexes in Unimolecular Decompositions. *Mass Spectrom. Rev.* **1988**, *7*, 363–393.
- Traeger, J. C.; Hudson, C. E.; McAdoo, D. J. Energy Dependence of Ion-Induced Dipole Complex Mediated Alkane Eliminations from Ionized Ethers. *J. Phys. Chem.* **1990**, *94*, 5714–5717.
- Frisch, M. J.; Trucks, G. W.; Schlegel, H. B.; Scuseria, G. E.; Robb, M. A.; Cheeseman, J. R.; Zakrzewski, V. G.; Montgomery, J. A., Jr.; Stratmann, R. E.; Burant, J. C.; Dapprich, S.; Millam, J. M.; Daniels, A. D.; Kudin, K. N.; Strain, M. C.; Farkas, O.; Tomasi, J.; Barone, V.; Cossi, M.; Cammi, R.; Mennucci, B.; Pomelli, C.; Adamo, C.; Clifford, S.; Ochterski, J.; Petersson, G. A.; Ayala, P. Y.; Cui, Q.; Morokuma, K.; Malick, D. K.; Rabuck, A. D.; Raghavachari, K.; Foresman, J. B.; Cioslowski, J.; Ortiz, J. V.; Baboul, A. G.; Stefanov, B. B.; Liu, G.; Liashenko, A.; Piskorz, P.; Komaromi, I.; Gomperts, R.; Martin, R. L.; Fox, D. J.; Keith, T.; Al-Laham, M. A.; Peng, C. Y.; Nanayakkara, A.; Challacombe, M.; Gill, P. M. W.; Johnson, B.; Chen, W.; Wong, M. W.; Andres, J. L.; Gonzalez, C.; Head-Gordon, M.; Replogle, E. S.; Pople, J. A. Gaussian, Inc.: Pittsburgh, 1998.
- Zhu, T. L.; Hase, W. L. A General RRKM Program, *Quantum Chemistry Program Exchange*; Chemistry Department, University of Indiana: Bloomington, QCPE 1993; p 644.
- Scott, A. P.; Radom, L. Harmonic Vibrational Frequencies: An Evaluation of Hartree-Fock, Møller-Plesset, Quadratic Configuration Interaction, Density Functional Theory, and Semiempirical Scale Factors. *J. Phys. Chem.* **1996**, *100*, 16502–16513.
- Bowers, M. T.; Jarrold, M. F.; Wagner-Redeker, W.; Kemper, P. R.; Bass, L. M. Kinetics of Ion-Molecule Collision Complexes in the Gas Phase. *Faraday Dis. Chem. Soc.* **1983**, *75*, 57–76.
- Booze, J. A.; Schweinberg, M.; Baer, T. Transition State Structures and Angular Momentum Effects in the Dissociation Dynamics of Energy-Selected $C_4H_8^+$ Ions. *J. Chem. Phys.* **1993**, *99*, 4441–4454.
- Baer, T. The Structure, Energetics, and Dynamics of Organic Ions. Baer, T.; Ng, C.-Y.; Powis, I., Eds.; John Wiley and Sons: New York, 1996; 136.
- Morton, T. H. The Reorientation Criterion and Positive Ion-Neutral Complexes. *Org. Mass Spectrom.* **1992**, *27*, 353–368.